Characteristics of phospholipid vesicles enhanced by adhesion on an annular region

Janja Majhenc* and Bojan Božič
Institute of Biophysics, Faculty of Medicine, University of Ljubljana, Vrazov trg 2, SI-1000 Ljubljana, Slovenia

(Received 20 June 2018; revised manuscript received 19 March 2019; published 28 May 2019)

Phospholipid vesicle membranes are simple models used to study the mechanical properties of cell membranes. The shapes of flaccid vesicles can exhibit very diverse forms. When researching very flaccid vesicles, axisymmetrical vesicles with the membranes adhered to an annular region can also be observed. A phase diagram of such shapes was studied for different values of the vesicle parameters, i.e., the adhesion constant, the vesicle volume-to-membrane ratio, the volume ratio between the polar and the equatorial parts, and the equilibrium difference between the membrane monolayers. The energies of the annular shapes with respect to the vesicle parameters were closely examined and compared with the energies of the discocyte and stomatocyte shapes. The requirements for the existence of such annular shapes were also given for adhesion-free vesicle membranes. The results show that the adhesion between the lipid bilayers stabilizes the observed shapes, which belong to the locally stable branch of the annular vesicles. The value obtained for the adhesion constant of the SOPC membrane is $3 \times 10^{-9}\,\mathrm{J/m^2}$.

DOI: 10.1103/PhysRevE.99.052416

I. INTRODUCTION

The mechanical attachment between cells is an essential feature of many biological processes, e.g., wound healing, immune response, and cell recognition [1]. Cell adhesion is normally a consequence of certain proteins, which can bind only through specific ligands to surfaces that have the appropriate receptors. These ligands can be organized in different patterns on the membrane [2]. If the ligands are homogeneously doped in the membrane or if a prevailing interaction is caused by the lipid molecules, the term nonspecific adhesion is often introduced to describe the membrane adhesion [3,4], like the adhesion between red blood cells in the presence of dextran [5]. The adhesion between two cells or lipid vesicles can induce the formation of doublets and affects their conformation [5–7]. Adhesion can also group together a number of cells or vesicles into a rouleau [5,8].

Vesicles are appropriate models for studying nonspecific adhesion [3]. Since they are prepared in the laboratory, the composition of the membrane and the surrounding solutions can be accurately determined. The first step of vesicle formation is usually the depletion of the lipid bilayer from the lipid stack, i.e., the transition from the adhered or bound state to the free state. If attractive forces prevail over repulsive ones, the system is in the bound state [9,10]. When vesicles are formed, their shapes depend on the membrane's area, volume, and composition, as well as on additional external forces. For small reduced volumes the shapes of the vesicles can be very diverse. The reduced volume is the ratio between the volume of the vesicle and the volume of the sphere with the same area as the area of the vesicle membrane. The classes of vesicle shapes were extensively studied and arranged into phase diagrams of axisymmetrical [11,12] and nonaxisymmetrical shapes, e.g., starfish vesicles [13]. Theoretically, the shapes can be determined by an energy minimization [11,14].

Any interactions between the vesicle and the surroundings can change the shape of vesicle. Therefore the vesicles with low reduced volume can be used to study adhesion. A variety of different shapes of vesicles adhered to a flat substrate have been determined for free [3] or tethered [15] vesicles. The conditions needed for a vesicle to be bound to a substrate also were discussed [9].

If the substrate is elastic, there are different wrapping states depending on the adhesion and the bending stiffnesses [16]. Since the shape of the substrate can be changed, these systems can behave in a similar way to the adhesion between cells. The shapes of the vesicles adhered to transparent substrate were assessed experimentally with a confocal microscope [17]. Using modulating adhesion of charged giant vesicles to a planar substrate enables researchers to perform reversible sets of experiments on the same vesicle and to compare different methods to determine adhesion constants [17].

For reduced volumes below 0.5, parts of the vesicle's membrane can be in contact, which gives us the possibility to study adhesion between parts of the inner monolayer of the same membrane. The shape of such a vesicle is governed only by adhesion and bending energies, without any spatial or elastic restrictions because of the substrate. In the axisymmetrical class of shapes, such shapes are the torocyte and codocyte [18,19]. Although the inner solution of torocytes and codocytes adapts a toroidal shape, the membrane of such vesicles possesses a spherical topology, so there is one volume and one membrane.

The adhered part of the membrane can divide the vesicle volume into two parts. The membrane material can pass through the adhered part, but the inner vesicle solution cannot pass through it. There is still one membrane of the vesicle, even though there are two separate volumes. In the class of axisymmetric shapes, the adhered regions have to be annular,

*janja.majhenc@mf.uni-lj.si

so such vesicles can be referred to as annular vesicles. We can define three distinct parts of the vesicle. The polar part is surrounded by the adhered part, and the latter is surrounded by the equatorial part.

In this paper we analyze the axisymmetrical phospholipid vesicles with adhesion on the annular part of the membrane. In Sec. II a description of the experimental design is given. The relevant energy terms for the determination of the annular shapes are given in Sec. III, while the corresponding boundary conditions are given in Appendix A. In Sec. IV we study the influence of the vesicle parameters and adhesion characteristics on the annular shapes that are mapped in the phase diagram. We find that the both continuous and discontinuous shape transitions are possible. Appendix B provides derivation of the differential equations and corresponding boundary conditions for the different adhesion characteristics.

II. EXPERIMENT

Vesicles were prepared from SOPC (1-stearoyl-2-oleoyl-sn-glycero-3-phosphocholine), obtained from Avanty Polar Lipids, in 0.2 M glucose solution. Lipid was used as purchased. To obtain a high fraction of vesicles with low reduced volumes the spontaneous swelling method was used [18,20]. After a foggy cloud appeared above the Teflon disk, lipid was gently scraped off the disk with a spatula to obtain vesicles with prolonged shapes, i.e., shapes with low reduced volume and large difference between the outer and inner membrane monolayer. Just before observation a small amount of vesicle solution was mixed with isomolar glucose solution in the ratio 1:2 v/v to induce a decrease of the equilibrium area difference [18]. This decrease is more pronounced if the lipid stock solution was freshly prepared from the powder. The sample was placed into a sealed chamber and observed with a phase contrast microscope.

Shape changes due to the decrease of the equilibrium areas difference were observed approximately 15–30 min after mixing the solutions. Annular-shaped vesicles are very rare and were found accidentally. The frequency of annular vesicles is comparable to the frequency of toroidal vesicles. Their shapes were not significantly changed during the period of the observation for about 30 min, therefore the shapes should be stable. Some shape variations were noticed, which can be associated with thermal fluctuations. The most pronounced mode changes the width of the equatorial part as indicated in Fig. 1.

The area and the volume, as well as the volume ratio between the vesicle parts, can be determined from the image only if the vesicle is in an appropriate orientation, assuming that the shape is axisymmetrical (Fig. 1). The center of the line was chosen as the membrane position. The experimental errors were determined from the differences of the estimated values.

III. THEORY

The shapes of the vesicles are determined by the minimum of the mechanical energy of the membrane [22]. This energy is composed of the membrane elastic energy and the adhesion energy that is a consequence of the interaction between the bilayers in the adhered part.

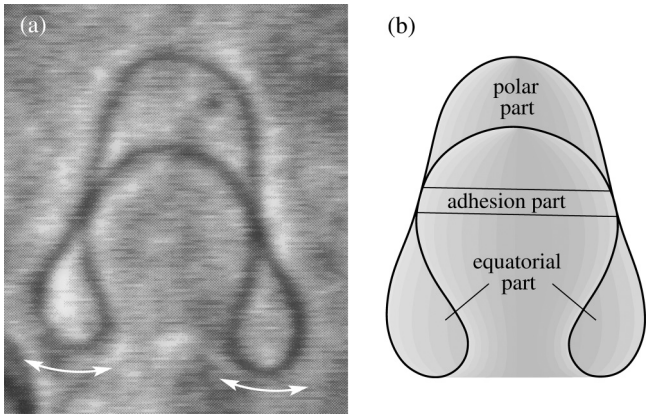

FIG. 1. (a) Image of the phospholipid vesicle with the adhesion on the annular region (annular vesicle) as observed using a phase-contrast microscope. Assuming an axial symmetry, the reduced volume of the observed vesicle is determined to be between 0.25 and 0.27, and the ratio between the polar and the equatorial parts of the volumes is between 0.37 and 0.42 [21]. The arrows indicate the direction of small fluctuations of the shape. (b) A representation of the theoretically obtained shape of the annular vesicle with the indicated longitudinal cross section and vesicle parts.

The membrane elastic energy can be well described by the area-difference-elasticity (ADE) model [23], within which the relevant energy terms for the description of the vesicle behavior are the local

$$E_{\mathrm{b}} = \frac{k_{\mathrm{c}}}{2} \oint (C_1 + C_2 - C_0)^2 \, dA \tag{1}$$

and the nonlocal

$$E_{\mathrm{r}} = \frac{k_{\mathrm{r}}}{2Ah^2} (\Delta A - \Delta A_0)^2 \tag{2}$$

bending terms, where k_{c} and k_{r} are the local and the nonlocal bending constants, C_1 and C_2 are the principal curvatures, C_0 is the spontaneous curvature of the membrane, A is the membrane area, h is the distance between the neutral surfaces of the outer and the inner monolayers, ΔA is the difference between the areas of the neutral surfaces of the two monolayers, and ΔA_0 is the corresponding equilibrium area difference. The principal curvatures are reciprocal to the principal radii ($C_j = 1/R_j$, $j = 1, 2$). The difference between the areas of the monolayers depends on the vesicle shape, whereas the difference between the equilibrium areas of the two layers is determined by the number of phospholipid molecules composing the monolayers and by the area of phospholipid molecules at equilibrium. In the presented analysis the ratio between the bending constants is taken to be three, i.e., $k_r/k_c = 3$ [18,24].

The interaction between the bilayers can be, for nonspecific adhesion, taken into account by adding to the elastic energy the energy term [3]

$$E_w = -wA_w, \tag{3}$$

where w is the adhesion constant and A_w is the area of the double bilayer vesicle region.

Since the vesicle is divided into three parts, i.e., the polar part, the annular part, and the equatorial part, the vesicle membrane also has to be divided into the corresponding regions to

determine the annular shape. Using the boundary conditions, which also include the membrane adhesion, at the regions, the system of differential equations has to be solved for each part [Appendix A, Eqs. (A14)]. The change of the meridian curvature of the membrane at the rim of the adhered region is proportional to the square root of the adhesion constant.

For the sake of simplicity all vesicle dimensions are given relative to the radius of the sphere that has the same area as the area of the vesicle membrane $R_0 = \sqrt{A/4\pi}$. Similarly, the reduced volume, the reduced equilibrium area difference, and the reduced contact area are defined as $v = 3V/4\pi R_0^3$, $\Delta a_0 = \Delta A_0/8\pi h R_0$, and $a_w = A_w/4\pi R_0^2$, respectively. If the adhesion energy is comparable to the local bending energy, it is appropriate to measure the energy terms relative to the bending energy of the sphere ($8\pi k_c$). Accordingly, the reduced total energy is then given by $e = (E_b + E_r + E_w)/8\pi k_c$. Additionally, the reduced adhesion constant (W) and the reduced pressure (M_i) are introduced with the equations (see Appendix A)

$$W = \frac{R_0^2}{2k_c} w, \tag{4}$$

$$M_i = \frac{R_0^3}{6k_c} \Delta p_i, \tag{5}$$

where Δp_i is the difference between the pressure in the corresponding vesicle part and the pressure in the surroundings. The index i denotes the different parts of the vesicle.

The introduction of the reduced adhesion constant is convenient for theoretical predictions. If it is large ($W \gg 1$), the contribution of the bending energy is almost negligible, and the vesicle shape attains a maximal adhered area at given geometry constraints. The main features of these vesicle shapes are high membrane curvatures at the rim of the adhered region whereas the membrane is tensed. If the curvatures at the rim are small, the adhesion energy is comparable to the bending energy and the membrane tension is small.

The visible average area of the vesicle membrane is smaller than the total one due to the thermal fluctuations [25,26]. The hidden area depends on the membrane tension. For low membrane tensions (lower than 2 mN/m) the changes of the hidden area do not exceed 2% of the membrane area [26], which is within the range of our experimental errors. As observed annular vesicles have low membrane curvatures, the membrane tension is low. Therefore we consider the visible membrane area as a constant. The relative volume of the observed vesicle corresponds to the visible membrane area.

IV. RESULTS AND DISCUSSION

A. Phase diagram

The results presented are restricted to axisymmetrical vesicles involving a contact area that exists only at low values of the reduced volume. Their shapes depend on the reduced volume (v) and on the reduced equilibrium difference between the membrane monolayers (Δa_0) for a given ratio between the bending constants (k_r/k_c) and a given adhesion constant (w) [18]. For annular vesicles the phase space of the shapes has one additional dimension, since the adhesion on the annular region prevents the exchange of the solution between the polar and the equatorial parts of the vesicle. Namely, the ratio between the volumes of the polar and the equatorial regions ($\rho = V_1/V_3$) remains constant. For this reason it is reasonable to show a phase diagram of the annular vesicles, for a given reduced volume and the reduced adhesion constant (W), as a function of the ratio ρ and the area difference Δa_0 (Fig. 2).

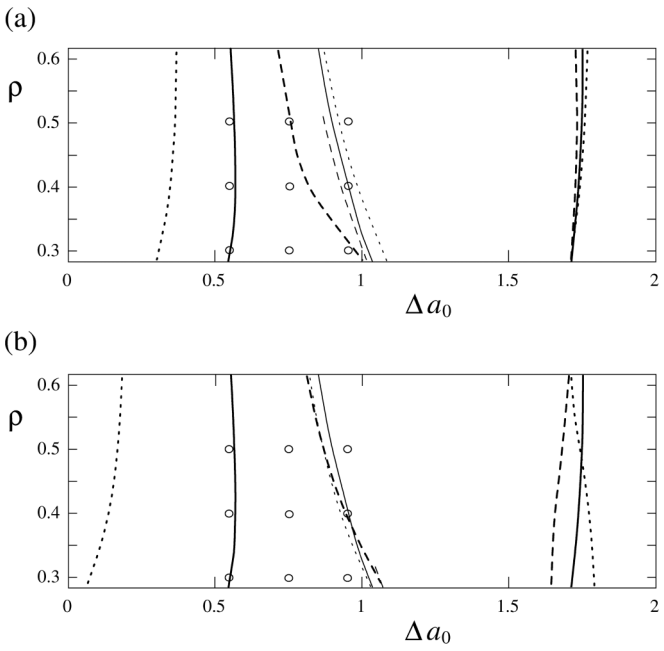

FIG. 2. The ρ-Δa_0 phase diagram of annular phospholipid vesicles as a function of the volume ratios between the polar and equatorial parts (ρ) and the reduced equilibrium area difference (Δa_0). The left-hand boundary lines represent the limiting shapes, where the area of the adhered ring is infinitesimally small, and the right-hand boundary lines represent the limiting shapes with the closed neck of the polar region. The thin lines represent a discontinuous transition of the polar part shape. The boundary lines are presented in panel (a) for three reduced adhesion constants [$W = 0.7$ (dotted lines), 1.0 (full lines), and 1.4 (dashed lines)] at the reduced volume $v = 0.25$ and in panel (b) for three reduced volumes [$v = 0.2$ (dashed lines), 0.25 (full lines), and 0.3 (dotted lines)] at the reduced adhesion constant $W = 1$. The small circles indicate the positions in the phase diagram for the shapes in Fig. 3.

The shapes with the annular adhered region exist for the parameters between the boundary lines shown in Fig. 2. The left-hand boundary line represents the limiting shapes, where the area of the adhered annular region is infinitesimally small. For any smaller Δa_0 at a given ratio ρ there is neither an adhered region nor a volume separation. The right-hand boundary line represents the limiting shapes with the closed neck of the polar region. When the neck of the polar region is closed, the shape of the polar part is spherical. As a sphere has, for a given volume, the smallest area, there is the maximum membrane area for the adhered region. On increasing Δa_0 beyond the right-hand boundary, the annular shape remains almost the same, while the membrane tension increases. As expected, because the limiting shapes are similar at this boundary, the influence of the adhesion constant on the Δa_0 values is not significant for this limit. The influence of the adhesion constant on the vesicle shape is more important at

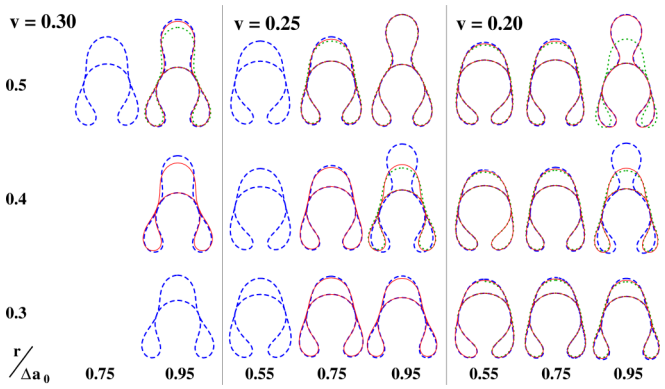

FIG. 3. Cross sections of the axisymmetrical shapes of the annular vesicles presented in groups for the reduced volumes 0.3 (left panel), 0.25 (middle panel), and 0.2 (right panel). The shapes presented in the upper, middle, and lower rows correspond to the volume ratio ρ, equal to 0.3, 0.4, and 0.5. The shapes presented in the columns correspond to the reduced area difference Δa_0, equal to 0.55, 0.75, and 0.95. The different line patterns correspond to the relative adhesion constant, equal to 0.7 (dotted line), 1.0 (full line), and 1.4 (dashed line).

lower Δa_0 values. The larger is the adhesion constant and the smaller is the reduced volume of the vesicle, the lower are the Δa_0 values at the left-hand limit, and therefore the part of the phase diagram where annular shapes exists is wider (Fig. 2).

In Fig. 3 the theoretical predicted shapes of annular vesicles are presented in three groups for three different reduced volumes. Different line patterns indicate different values of the adhesion constants. The position of a shape in a group indicates certain values of the parameters ρ and Δa_0 corresponding to the point in the phase diagram. The values of the parameters are chosen in such a way that the calculated shapes are similar to the observed one [Fig. 1(a)]. It should be noted that some shapes (for low values of W, ρ, and Δa_0, and for large values of v) are missing since the corresponding parameters of these shapes are outside the region of the phase diagram where the annular shapes exist.

It is clear from Fig. 3 that on increasing Δa_0 the equatorial part becomes wider, whereas the polar part becomes narrower and eventually forms a neck. The formation of the neck depends on the values of the constant W, the volume v, and the ratio ρ. The shape transformations and the neck formation can be continuous for larger values of the adhesion constant if the reduced volume and volume ratio are large. For smaller values of these parameters (w, v, and ρ) a discontinuous transformation of the shape occurs, i.e., an abrupt neck formation. For instance, for the reduced area difference Δa_0 equal to 0.95 and the ratio ρ equal to 0.4, the shapes for $W = 1$ and 1.4 are quite different. Namely, it is evident that the shape for $W = 1$ has a polar region with a neck. The exact locations of the discontinuous shape transformations are presented in the phase diagrams (the thin lines in Fig. 2).

Inspecting the shapes in Fig. 3 it is clear that the variation of the adhesion constant in some regions of the phase diagram has no significant influence on the vesicle shape, while in the other parts, particularly near the shape transition, the change in the adhesion has a crucial influence on the shape.

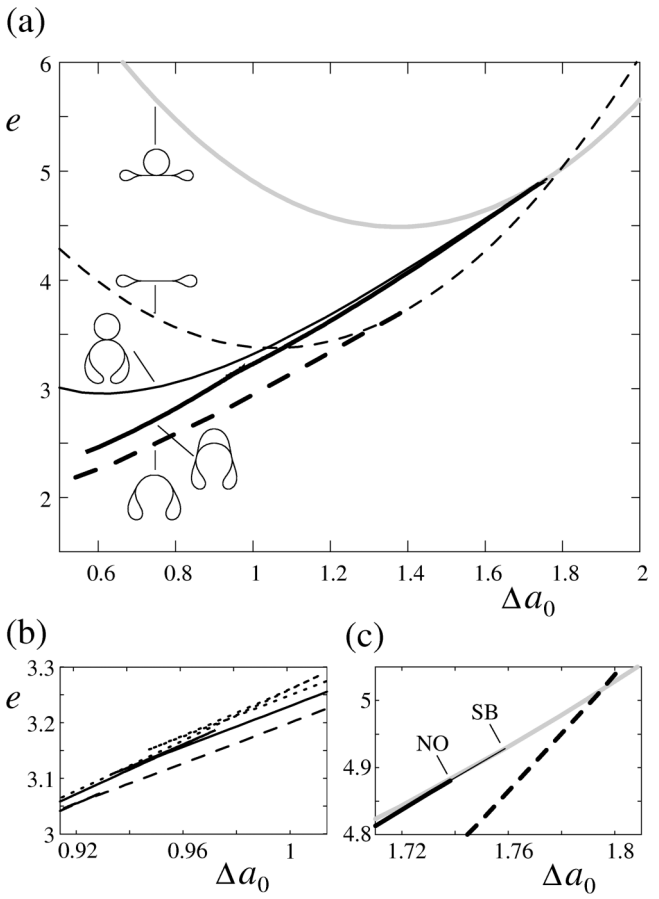

FIG. 4. (a) Dependence of the reduced total energy (e) as a function of the reduced equilibrium area difference (Δa_0) at $W = 1$, $v = 0.25$, and $\rho = 0.4$ for the annular and polar shape groups (solid and dashed lines). For class illustrations the shapes for $\Delta a_0 = 0.75$ are shown. The annular classes are the following: the shapes with the closed neck of the polar part and with the equatorial part having mirror symmetry (gray line), the shapes with the closed neck of the polar part and with the equatorial part having broken symmetry (thin solid line), and the shapes with the open neck of the polar part (thick solid line). The thin and the thick dashed lines represent the discocytes and the stomatocytes. (b) The energy e of the annular vesicle with the open neck of the polar part at the transition for reduced adhesion constants (W) equal to 0.7, 1.0, and 1.4. (c) The energies e for different branches of the shapes at large Δa_0. Bifurcation points on annular branch are indicated: (SB) broken mirror symmetry of the equatorial part and (NO) the neck opening of the polar part.

B. Energy

For given values of the parameters, the shapes of vesicles with the adhered area belong to different shape classes. The representative shapes of the classes are shown in Fig. 4. The classes are divided into two major groups, i.e., the annular and polar groups, depending on whether the vesicle volume is divided by the adhered region or not. The polar shape group contains stomatocyte and discocyte vesicles with the adhered area between the polar regions of the membrane. The annular

shape group contains (1) the shapes with the closed neck of the polar part and with the equatorial part having mirror symmetry, (2) the shapes with the closed neck of the polar part and with the equatorial part having broken symmetry, and (3) the shapes with the open neck of the polar part.

Energies for different branches of the shapes at large Δa_0 are shown in Fig. 4(c). It is clear that for Δa_0 larger than 1.795 the energy of the annular vesicles that possess a spherical polar part and an equatorial part having mirror symmetry is lower than that of the discocyte vesicle. However, on decreasing Δa_0 within the annular shape group, two shape transitions occur. First, the symmetry of the equatorial part breaks (SB) and then the neck of the polar part opens (NO). The line describing the energies of the annular vesicles with the open neck ends where the adhered area becomes infinitely small (left-hand boundary on the phase diagram, Fig. 2). To see the transition between the shape classes the energies are presented for all classes of shapes.

The energies of the discocyte or stomatocyte shapes are lower than the annular shapes counterparts, except for high values of the equilibrium area difference ($\Delta a_0 > 1.75$). Therefore a spontaneous transition from stomatocyte to annular shape at lower area differences is not possible. We can speculate that the annular vesicle with the open neck of the polar part can be formed in two steps. First, a vesicle with a low reduced volume and a large Δa_0 is formed, where the vesicle volume can be divided into two parts by the adhesion of the membrane. Second, on decreasing Δa_0 the vesicle remains on the annular branch of the shapes, even though the neck opens. As the conditions for the formation of annular vesicles, i.e., the low v concomitantly with large Δa_0, are so extreme, such vesicles are not observed frequently.

C. Neck formation

A vesicle with or without a neck is the result of a competition between the bending and the adhesion energy. The formation of the neck increases the local bending energy [Eq. (1)] as the curvatures are higher. However, the neck formation can also decrease the nonlocal bending energy [Eq. (2)], if the area difference of the shape (ΔA) is closer to the equilibrium area difference (ΔA_0). During the formation of the neck the polar part becomes more spherical, meaning that more membrane area can be in the adhered part. A larger adhered area implies a lower adhesion energy [Eq. (3)]. Therefore, the adhesion favors the neck formation. For larger values of the adhesion constant, the shapes with a neck occur at lower values of the reduced equilibrium area difference (Δa_0), as can be seen in Fig. 4(b).

Due to the competition between the bending and adhesion energies, for a relatively small range of parameters, more than one solution to the system of differential equations [Appendix A, Eq. (A14)] can exist, even in the class of annular shapes with the open necks. The range of Δa_0 where more than one solution can exist is larger when the adhesion is smaller, since to overcome the bending energy more adhered area is needed [Fig. 4(b)]. A stable shape is the shape with the lowest energy. The energy dependence of the annular vesicles on Δa_0 suggests that the different solutions should be quite similar in shape. However, the area of the adhered membrane changes significantly in the same range of Δa_0. It experiences a sigmoidal dependence of the adhered area on Δa_0 at the transition (Fig. 5). Considering only the solutions with the smallest energy (indicated by the thick lines in Fig. 5), a large shape difference or discontinuous transition is predicted. The smaller is the adhesion constant, the larger is the difference in the adhered areas and the larger is the shape change [27]. The width of the adhered ring is almost proportional to the adhered area since the radius of the ring does not change significantly (Fig. 3).

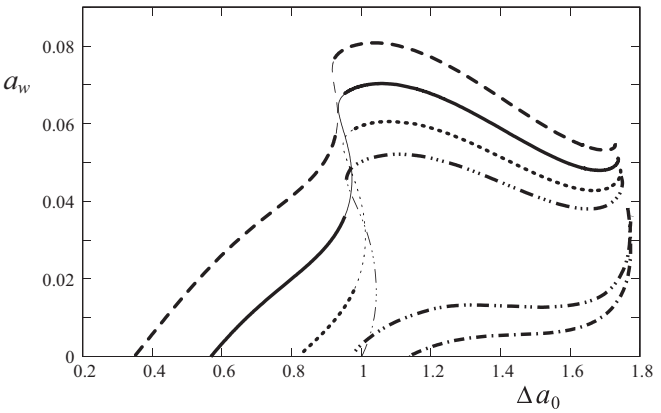

FIG. 5. Dependence of the reduced area of the adhered part ($a_w = A_w/A$) on Δa_0 for six values of the reduced adhesion constant (W) 1.4, 1, 0.7, 0.497, 0.015, and 0 (dashed, full, dotted, dash-three dots, dash-two dots, and dash-dot lines) at $\rho = 0.4$ and $v = 0.25$. The thick lines represent the dependencies for the stable annular vesicles, i.e., shapes with the minimum total energies.

For smaller adhesion constants the discontinuous transition occurs at larger Δa_0 and a larger Δa_0 is needed for the existence of the annular vesicle shapes [Fig. 2(b)]. Thus, for the small adhesion constant, only the shapes with a neck in the polar part exist.

For certain combinations of the reduced volumes and volume ratios there is a narrow range of adhesion constant, where more than one solution for the annular shape exists; however, the solution without neck is not stable. In these cases, the annular shapes with a finite area of the adhered region exist at the left-hand boundary (Fig. 5). For example, at the reduced volume 0.25 and the volume ratio 0.4 this range of the adhesion constant is between 0.015 and 0.497, while the reduced adhered area (a_w) of the shapes at this boundary varies from zero to 0.046 and the corresponding width of the adhered region varies from zero to $0.2R_0$. In all other cases, the adhered region of the limiting shapes is infinitesimally thin at the left-hand boundary.

Any opening of the adhered ring will induce the discontinuous shape transition to the stomatocyte shape, as they have lower energies than annular shapes at given Δa_0 values. The energy needed to open the adhered ring is determined by the difference between the energy of the stable vesicle at given Δa_0 and the energy of the vesicle at the same Δa_0 attaining the limiting shape. Comparing this energy difference to the thermal energy (k_BT with k_B the Boltzmann constant and T the temperature) gives the minimal width of the adhered ring needed to prevent the opening. The width of the ring depends

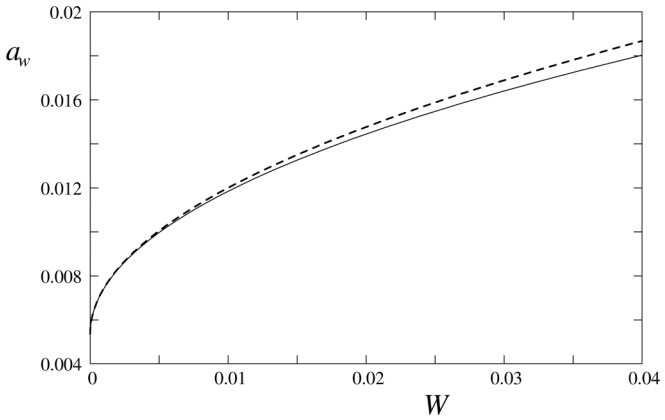

FIG. 6. The dependence of the reduced contact (adhered) area (a_w) on the reduced adhesion constant (W) at $\Delta a_0 = 1.4$, $\rho = 0.4$, and $v = 0.25$. The contact area is finite (a_{w0}) even at zero adhesion constant. The full line is obtained by solving the system of differential equations. The dashed line represents the expression $a_{w0} + \kappa\sqrt{W}$ where κ is adjusted to fit the theoretically obtained values at small adhesion constants.

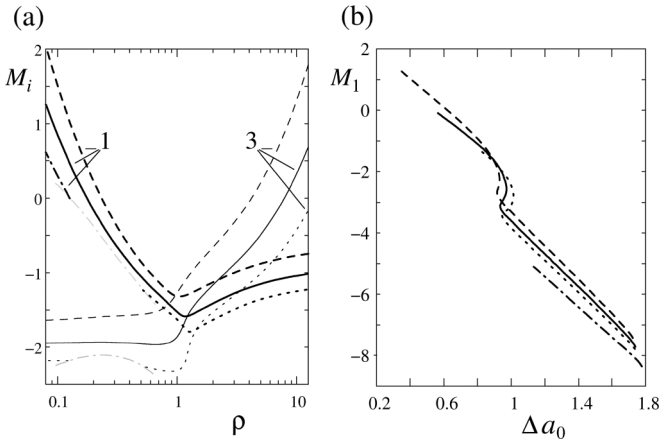

FIG. 7. (a) The reduced pressure differences between the inside and the outside of the vesicle for the polar and equatorial parts (M_i) as a function of the volume ratio for these parts (ρ) for three values of the adhesion constant 0.7 (dotted lines), 1 (full lines), and 1.4 (dashed lines) at $\Delta a_0 = 0.75$ and $v = 0.25$. The curves denoted by 1 and 3 correspond to the polar and equatorial parts, respectively. The thin dash-dot lines show the limit at which the area of the annular part is zero. (b) The reduced pressure differences between the inside and outside of the polar vesicle part (M_1) as a function of reduced equilibrium area difference (Δa_0) for four values of the adhesion constant 0 (dash-dot line), 0.7 (dotted lines), 1 (full lines), and 1.4 (dashed lines) at $\rho = 0.4$ and $v = 0.25$.

on the reduced adhesion constant (W). For the values of W equal to 0, 0.7, 1, and 1.4 the corresponding minimal values of a_w are 0.00118, 0.00277, 0.00350, and 0.00574. This increase in a_w on W is not intuitive. The ring is wider, because at a larger adhesion constant the opening occurs at lower Δa_0. Namely, for any annular shape at given adhesion constant, Δa is smaller than Δa_0 and their difference is larger at larger Δa_0. Consequently, a smaller increase of Δa_0 is needed at larger Δa_0 for the same energy increase [Eq. (2)]. Therefore a smaller increase of Δa_0 is reflected in a smaller adhered area and a narrower ring (Fig. 5). The demand for the finite width of the ring affects the phase diagram since the left-hand boundary moves to larger Δa_0 values. This shift is small since the range of Δa_0 values, where annular vesicles exist, is reduced for less than 5% .

D. The behavior at small adhesion

The results in Fig. 5 clearly show that at small values of Δa_0 the annular shapes exist only at appropriate values of adhesion. In contrast, at large values of Δa_0 the annular shapes exist even without adhesion, i.e., at zero values of W. The dependence of the reduced contact area on the reduced adhesion constant at large values of Δa_0 in Fig. 6 shows that the contact area continuously increases with increasing adhesion. The question to be posed is: what is the power law for these dependencies? The answer is in the boundary conditions that connect the meridian membrane curvature with the adhesion constant [Appendix A, Eqs. (A17)–(A20)]. The Taylor series for the meridian curvatures of the two adjacent membranes close to the arc length connecting point at zero adhesion (s_0) are

$$c_{m,i} = c_{m,0} + \frac{\mathrm{d}c_{m,i}}{\mathrm{d}s}(s - s_0) + \cdots , \tag{6}$$

where $c_{m,0}$ is the meridian curvature of the membrane at the border of the annular part. Equation (6) shows that in a first approximation the difference in the membrane curvature is proportional to the membrane's arc length, which is proportional to the change in the adhered area. However, on increasing the adhesion constant, the change in the membrane curvatures of the two adjacent membranes is proportional to the square root of this constant. Therefore, the increase in the adhered membrane area ($a_w - a_{w0}$, where a_{w0} is the contact area at zero adhesion constant) is approximately proportional to the square root of the adhesion constant. The corresponding square root function is also shown in Fig. 6.

E. Pressure

Generally, the total volume of the closed phospholipid membrane is constant due to the osmotic conditions. Consequently, the pressure inside the vesicle is not the same as the pressure in the vesicle's surroundings. Because the adhesion on the annular region disables the solvent transport between the polar and equatorial parts of the vesicle, the volumes of both parts are fixed. Therefore, the pressures in these parts are generally different, whereas the membrane lateral tension varies over the vesicle regions [28], and the pressure difference across the membrane (Δp_i) is uniform at the individual vesicle part.

Figure 7(a) shows the reduced pressures of both parts of vesicles as a function of the volume ratio of these parts (ρ) for different values of the reduced adhesion constant where the total volume of the vesicle is fixed. It is clear that the pressure inside the polar part is large for small ratios ρ, and similarly, the pressure inside the equatorial part is large for large ratios ρ. Concomitantly, the changes in pressure inside the larger parts are relatively small. In addition, a larger adhesion causes larger pressures in both vesicle parts.

The curvatures at the vesicle poles depend on the properties of the whole vesicle. The change in the membrane curvature at the rim of the polar part is dependent on the adhesion constant [Appendix A, Eqs. (A17)–(A20)]. For a small vesicle part the change in the curvature from its value between the pole to the rim occurs at a small distance. Also in the case of a small equatorial part the change of membrane curvature occurs at a small distance. As the pressure is proportional to the derivative of the membrane curvature, the pressure in the small vesicle part is high.

The pressure differences across the membrane also depend on Δa_0. In Fig. 7(b) the pressure difference at the polar part is shown as a function of Δa_0 for the same values of the adhesion constant as in Fig. 7(a). It is evident that the pressure difference decreases with increasing Δa_0.

With increasing Δa_0 the pressure in the polar part decreases, since this part becomes more spherical. Namely, the sphere has the smallest possible area at a given volume, and the excess of the membrane area causes the pressure to decrease in the polar region. Similarly, the excess of the membrane area is also reflected in the pressure decrease in the equatorial region (not shown).

The adhesion between the membrane parts tends to increase the adhered area. Therefore, the adhesion increases the range of parameter values, e.g., the interval of the equilibrium area difference (Figs. 2 and 7) at which the annular shapes exist. For the same reason, besides the interval of Δa_0 values the adhesion also increases the interval of the ρ values. In addition, for larger adhesion the tendency to diminish the membrane areas of the polar and equatorial vesicle parts causes an increase in the lateral tension and, consequently, the pressure inside these parts (Fig. 7).

F. Relevance of the adhesion energy

The interaction of the membrane that is in contact with another membrane is complex. It is often assumed to be composed by the van der Waals attraction $[(H/12\pi)[1/Z^2 - 2/(Z+D_B)^2 + 1/(Z+2D_B)^2]$, with D_B being the bilayer thickness, Z being the distance between the membranes, and H being the Hamaker parameter, typically of the order of magnitude 10^{-22} to 10^{-21} J], the hydration repulsion ($B_H e^{-Z/Z_H}$ with $B_H = 0.2$ J/m and $Z_H = 0.3$ nm), and the effective steric interaction resulting from the thermal undulations $[0.42(k_BT)^2/k_cZ^2]$ [9,29]. The listed expressions describe the interactions for flat tensionless membranes. The corresponding interaction potential between the membranes $[V(Z)]$ is distance dependent.

To find if the shape of a vesicle adhered to a firm flat surface significantly depends on the parameters of the interaction potential, we compare the predictions of the square well potential with the predictions of the simple energy model [expression (3)]. The square well potential $V(Z)$ is equal to ∞ for $Z < 0$, to $-\tilde{w}$ for $0 \leqslant Z \leqslant Z_0$, and to 0 for $Z_0 < Z$ where $\tilde{w}$ is the potential depth and Z_0 is the interaction distance [9,30]. In this case the corresponding energy term is written by the expression

$$E_{\tilde{w}} = -\tilde{w}A_{\tilde{w}}, \tag{7}$$

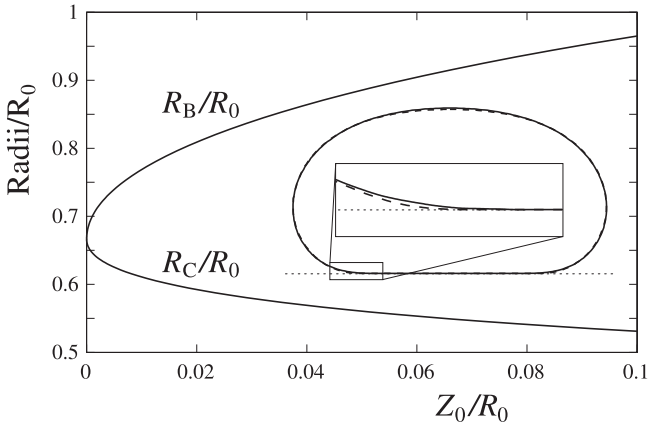

FIG. 8. The effect of the normalized interaction distance (Z_0/R_0) of the square well potential on the shape of the vesicle for $v = 0.9$ and $\tilde{W} = R_0^2\tilde{w}/2k_c = 1$. R_C is the radius of vesicle footprint on the surface, and R_B is the radius of the vesicle membrane at the interaction distance of the square well. Two representative vesicles shapes that correspond to $Z_0/R_0 = 0$ (dashed line) and 0.1 (full line) are also shown. The dotted line shows the reference plane of the surface. The inset shows the enlarged part of the vesicle shapes.

where $A_{\tilde{w}}$ is the membrane area located at the distances smaller than Z_0. The system of differential equations has to be solved in order to obtain the vesicle shape for the case, where the corresponding boundary conditions at Z_0 have to be taken into consideration (Appendix B).

Figure 8 shows how the radius of the vesicle footprint on the surface $[R_C = R(0)]$ and the radius of the vesicle membrane at the interaction distance of the square well $[R_B = R(Z_0)]$ approach to the contact radius of the simple model (R_S) [expression (3)] for $w = \tilde{w}$. The corresponding differences ($R_S - R_C$ and $R_B - R_S$) are proportional to $Z_0^{0.5}$.

The differences between the shapes predicted by the square well model and the simple model can be noticed in the vicinity of the boundary of the adhered membrane as seen in the enlarged section in Fig. 8. Since the interaction distance Z_0 is in the range of nanometers and the typical size of vesicle is several micrometers ($Z_0/R_0 \sim 10^{-3}$), the differences between shapes, predicted by the models, are small. As the scope of this work is to determine a global shape of the vesicle, a simple model of contact adhesion can be used. It has to be emphasized that the value of the adhesion constant used in the simple model should be considered as an effective one, which corresponds to the minimum of the interaction potential $[V(Z)]$.

G. The estimation of the adhesion constant

The most noticeable shape change that depends on the adhesion constant is the transition between the shapes with and without a neck. Moreover, for small or no adhesion the annular shapes exist only at large equilibrium area differences, where the shapes are characterized by the polar part having a neck. As the observed shape had no neck, it follows that the reduced adhesion constant cannot be smaller than 0.5 (Fig. 5). A more realistic estimation obtained by comparing the observed and calculated shapes is close to 1. This leads to

the conclusion that effective adhesion constant at the room temperature should be close to $3 \times 10^{-9}\,\mathrm{J/m^2}$, considering the values for the radius of the vesicle $R_0 = 8.2\ \mu\mathrm{m}$ and the elastic bending constant $k_c = 1 \times 10^{-19}$ J. The obtained value of effective adhesion constant should be considered as an estimation, as the annular vesicles are so rarely observed that meaningful statistics cannot been made.

Similar values for the reduced adhesion constants ($W = 0.4$–3.5) were obtained to form flat-contact doublets [5]. It is to be noted that the minimum adhesion needed for a stable annular shape without neck is close to the minimum adhesion needed for the doublet formation. Also, it is found that DOPC/DOPG vesicles start to adhere to the flat substrate at adhesion constant $0.8 \times 10^{-9}\,\mathrm{J/m^2}$ [17].

A competition between the attraction and repulsion forces determines the transition between the bound and unbound state of lipid membranes in a lipid stack. Slightly different values of the parameters in the expressions for membrane interactions lead to significantly different estimations for the temperature at which an unbinding occurs. The unbinding of one lipid bilayer from the lipid stack is the first step of a vesicle formation. At room temperature the formation of SOPC vesicles by the spontaneous swelling procedure takes several days. If the vesicles are prepared at higher temperature, the formation of vesicles occurs within hours. This indicates that the relevant unbinding temperature is close to the room temperature. On the other hand, theoretical studies show that the repulsion caused by the thermal fluctuations cannot be simply superposed to van der Walls and hydration interactions and that the membrane tension can affect the unbinding temperature [9,29]. The membrane of the annular vesicle is not completely flat and tensionless, which can lead to an energetically favorable contact between the parts of the membrane at the room temperature. This feature is described by the contact energy term [Eq. (3)] of the simple model, where the model parameter (w) is the effective adhesion.

V. CONCLUSION

A class of low-volume vesicles shapes where the membrane is in contact with the annular region that divides the vesicle volume into polar and equatorial parts was observed and theoretically determined. The shape of the annular vesicle depends on four parameters: the ratio between the volumes of the vesicle parts, the ratio between vesicle volume and its membrane area, the equilibrium difference between the areas of the membrane monolayers, and the adhesion constant. Annular shapes exist only for vesicles at relatively low reduced volumes and limited values of the equilibrium area difference. Therefore the volume division can be eliminated by a small change in the reduced volume or by a small change in the equilibrium area difference even at the unchanged adhesion constant.

Three classes of annular vesicle shapes are predicted by theory: the shapes with the closed neck of the polar part and with the equatorial part with (1) or without (2) mirror symmetry, and the shapes with the open neck of the polar part (3). The observed vesicle corresponds to the last of these, i.e., the shape class with the lowest energy.

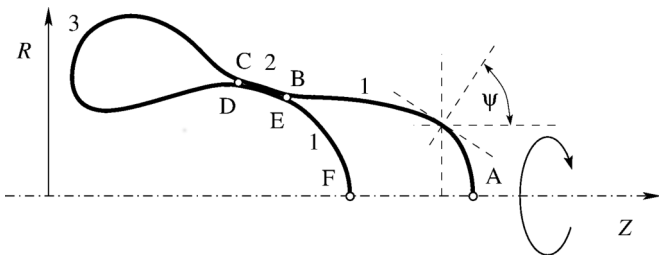

FIG. 9. Schematic presentation of an axisymmetric vesicle in cylindrical coordinates (Z and R) with a double bilayer region. The slope of the curvature is denoted by ψ. The polar, double bilayer, and equatorial region are denoted by numerals (1, 2, and 3), whereas the boundaries of these regions are denoted by letters (A, B, C, D, E, and F). The shape of the membrane is given by R and Z, the values of which are obtained by solving Eqs. (A14).

We propose a possible path for the shape development of the observed annular vesicle shape: division of the vesicle volume by the adhesion occurs at large Δa_0, and then on decreasing Δa_0 the vesicle remains on the annular branch of the shapes. Adhesion between the membrane parts increases the range of parameter values where the annular shapes exist. For a small adhesion between the membrane, the annular shape can exist only for larger equilibrium area differences, where the annular shapes are characterized by the polar part having a neck. As the observed shape had no neck, it follows that the estimated reduced adhesion constant is close to 1. To obtain the adhesion constant for SOPC membrane, recalculation to the dimensional adhesion constant (w) is necessary ($w = 2k_c W/R_0^2$) since the value of w depends only on the membrane compositions, which means that the effective adhesion constant at room temperature should be close to $3 \times 10^{-9}\,\mathrm{J/m^2}$. For this adhesion constant the predicted and the observed shapes are in good agreement.

ACKNOWLEDGMENT

This work was supported by the Slovenian Research Agency through the research program P1-0055.

APPENDIX A: DETERMINATION OF VESICLE SHAPES

We present a derivation of the system of differential equations and of the corresponding boundary conditions for the membrane shape of vesicles stuck in an annular region (Fig. 9). The equilibrium shapes are obtained by minimizing the mechanical energy under given conditions. It is convenient that all the vesicle dimensions are given relative to the radius of the sphere with the same surface area (A), $R_0 = \sqrt{A/4\pi}$, and that the energy terms are given relative to the bending energy of the sphere ($8\pi k_c$). The equilibrium states of the vesicle are the extremes of the mechanical energy (described in Sec. III, Theory) for a given volume of the polar and equatorial parts and the total membrane area. Therefore, the extremes of the mechanical energy that is composed of the membrane's local and nonlocal bending terms and the adhesion energy (E_b, E_r, E_w) correspond to the stationary points of the

functional [31]

$$g = e_b + e_r + e_w - \sum M_i v_i + La, \tag{A1}$$

where

$$e_b = \frac{1}{4}\oint (c_1 + c_2 - c_0)^2\, da \tag{A2}$$

is the reduced local bending energy ($e_b = E_b/8\pi k_c$),

$$e_r = \frac{k_r}{k_c}(\Delta a - \Delta a_0)^2 \tag{A3}$$

is the reduced nonlocal bending energy ($e_r = E_r/8\pi k_c$),

$$e_w = -W a_w \tag{A4}$$

is the reduced adhesion energy ($e_w = E_w/8\pi k_c$),

$$v_i = \frac{3V_i}{4\pi R_0^3} \tag{A5}$$

is the reduced vesicle volume of the polar or equatorial part, and

$$a = \frac{A}{4\pi R_0^2} = 1 \tag{A6}$$

is the reduced membrane area. The total vesicle reduced volume is given by $v = \Sigma v_i$. The reduced difference between the membrane monolayers (Δa), the reduced area of the annular region (a_w), the reduced adhesion constant (W), and the reduced principal and spontaneous curvatures (c_1, c_2, and c_0) are defined with

$$\Delta a = \frac{\Delta A}{8\pi h R_0}, \quad a_w = \frac{A_w}{A}, \quad W = \frac{wR_0^2}{2k_c},$$
$$c_1 = C_1 R_0, \quad c_2 = C_2 R_0, \quad c_0 = C_0 R_0, \tag{A7}$$

where the difference between the areas of the monolayers is given by the expression $\Delta A = h\oint (C_1 + C_2)\, dA$, with h being the distance between the membrane monolayers, A_w is the adhered area, and w is the adhesion constant. The constraints in volumes and the area are incorporated into the energy minimization by introducing the Lagrange multipliers $M_i = R_0^3 \Delta p_i/6k_c$ and $L = R_0^2\lambda/2k_c$, where Δp_i is the difference between the pressure in the vesicle particular part and the pressure in the vesicle surroundings, and λ describes how the energy responds to a change in the area. The lateral tension can be determined by the Lagrange multiplier fixing the whole vesicle area (L) and the membrane curvatures [28].

In the stationary point, the variation of the functional g with respect to the reduced equilibrium area difference (Δa_0) and to the arbitrary shape deviation is zero. The variation with respect to Δa_0 leads to the expression

$$N = -2\frac{k_r}{k_c}(\Delta a - \Delta a_0), \tag{A8}$$

where the parameter N represents the difference between the lateral tensions of the outer and inner monolayers.

The observed vesicles are axisymmetric; therefore, we can express the variation of the functional with respect to the shape in terms of an integral over the axisymmetric contour. An axisymmetric surface can be parameterized by the angle between the normal to the contour and the symmetry axis of the shape [$\psi(s)$] (Fig. 9), where s is the arc length along the contour in reduced units. The coordinates $r(s)$ and $z(s)$, which represent the distance between the symmetry axis and a point on the contour of the vesicle membrane and the position along the symmetry axis in reduced units, respectively, depend on ψ through $\dot{r} = \cos\psi$ and $\dot{z} = -\sin\psi$, where the dot denotes the derivation with respect to s. The reduced principal curvatures—the meridian and the parallel curvatures—are expressed by $c_m = \dot{\psi}$ and $c_p = \sin\psi/r$.

Six points on the contour with respect to the region boundaries are introduced: point A is the starting point, which lies at the pole of the vesicle; points B, C, D, and E are at the rims of the annular region that pertains to the double bilayer, but at two different radii and arc lengths; and point F is the ending point, which lies at the opposite pole of the vesicle (Fig. 9). Using integral expressions for the reduced volume, the reduced area and the reduced difference between the monolayer areas,

$$v = \frac{3}{4}\int_{\mathrm{A}}^{\mathrm{B}} r^2 \sin\psi\, ds + \frac{3}{4}\int_{\mathrm{C}}^{\mathrm{D}} r^2 \sin\psi\, ds + \frac{3}{4}\int_{\mathrm{E}}^{\mathrm{F}} r^2 \sin\psi\, ds, \tag{A9}$$

$$a = \frac{1}{2}\int_A^B r\, ds + \int_B^C r\, ds + \frac{1}{2}\int_C^D r\, ds + \frac{1}{2}\int_E^F r\, ds, \tag{A10}$$

and

$$\Delta a = \frac{1}{4}\int_A^B r\left(\frac{\sin\psi}{r} - \dot{\psi}\right) ds + \frac{1}{4}\int_C^D r\left(\frac{\sin\psi}{r} - \dot{\psi}\right) ds + \frac{1}{4}\int_E^F r\left(\frac{\sin\psi}{r} - \dot{\psi}\right) ds, \tag{A11}$$

we can express the variation of the functional g with respect to the shape as

$$\delta g = \delta\int_A^B \mathcal{L}_1\, ds + \delta\int_B^C \mathcal{L}_2\, ds + \delta\int_C^D \mathcal{L}_3\, ds + \delta\int_D^E \mathcal{L}_2\, ds + \delta\int_E^F \mathcal{L}_1\, ds, \tag{A12}$$

where the Lagrangian functions for the regions ($\mathcal{L}_i$, $i = 1$, 2, and 3) can be written as

$$\mathcal{L}_i = \frac{r}{8}\left(\frac{\sin\psi}{r} + \dot{\psi}\right)^2 - |i-2|N\frac{\sin\psi + \dot{\psi}r}{4} - (1 - |i-2|)\frac{W}{2}\frac{r}{2} - |i-2|M_i\frac{3r^2\sin\psi}{4} + L\frac{r}{2} + \Gamma(\dot{r} - \cos\psi) - F_i(\dot{z} + \sin\psi). \tag{A13}$$

The additional Lagrange multipliers $\Gamma(s)$ and $F_i(s)$ have to be introduced because the variables $r(s)$, $z(s)$ and $\psi(s)$ are interdependent. The index i is 1 when referring to the vesicle polar regions; it is 2 when referring to the vesicle double bilayer region, where parts of the membrane are in contact; and it is 3 when referring to the equatorial region of the vesicle. Since the double bilayer is composed of the two oppositely oriented bilayers belonging to the same membrane, the relative tension of one bilayer compensates for the relative

tension of the other and the pressure is the same at both sides of the double bilayer [Eq. (A13)].

The variation of the functional with respect to shape is zero ($\delta g = 0$) if the Euler-Lagrange equations [$\partial \mathcal{L}_i/\partial x_j = \frac{d}{ds}(\partial \mathcal{L}_i/\partial \dot{x}_j)$ with x_j the component of the vector of variables $\mathbf{x} = (r, \psi, z, \Gamma, F_i)$] and the boundary conditions are fulfilled. By performing the variation we obtain the following system of differential equations:

$$\begin{aligned}
\dot{\Gamma} &= \frac{1}{8}\left(\dot{\psi}^2 - \frac{\sin^2\psi}{r^2}\right) - |i-2|\frac{3M_i r\sin\psi}{2} \\
&\quad + \frac{L-(1-|i-2|)W/2}{2} - \frac{N\dot{\psi}}{4}, \\
\ddot{\psi} r &= \frac{\dot{r}\sin\psi}{r} - \dot{\psi}\dot{r} - 3|i-2|M_i r^2\cos\psi - 4F_i\cos\psi \\
&\quad + 4\Gamma\sin\psi, \\
\dot{F}_i &= 0, \\
\dot{r} &= \cos\psi, \\
\dot{z} &= -\sin\psi. \qquad \text{(A14)}
\end{aligned}$$

The boundary conditions obtained by the minimization procedure are described using the equation

$$\begin{aligned}
&-H_1\delta s\big|_{\mathrm{A}}^{\mathrm{B}} - H_2\delta s\big|_{\mathrm{B}}^{\mathrm{C}} - H_3\delta s\big|_{\mathrm{C}}^{\mathrm{D}} - H_2\delta s\big|_{\mathrm{D}}^{\mathrm{E}} - H_1\delta s\big|_{\mathrm{E}}^{\mathrm{F}} + \sum_j \frac{\partial \mathcal{L}_1}{\partial \dot{x}_j}\delta x_j\Big|_{\mathrm{A}}^{\mathrm{B}} \\
&+ \sum_j \frac{\partial \mathcal{L}_2}{\partial \dot{x}_j}\delta x_j\Big|_{\mathrm{B}}^{\mathrm{C}} + \sum_j \frac{\partial \mathcal{L}_3}{\partial \dot{x}_j}\delta x_j\Big|_{\mathrm{C}}^{\mathrm{D}} + \sum_j \frac{\partial \mathcal{L}_2}{\partial \dot{x}_j}\delta x_j\Big|_{\mathrm{D}}^{\mathrm{E}} \\
&+ \sum_j \frac{\partial \mathcal{L}_1}{\partial \dot{x}_j}\delta x_j\Big|_{\mathrm{E}}^{\mathrm{F}} = 0, \qquad \text{(A15)}
\end{aligned}$$

where

$$H_i = -\mathcal{L}_i + \dot{\mathbf{x}}\cdot\frac{\partial \mathcal{L}_i}{\partial \mathbf{x}} \qquad \text{(A16)}$$

are the Hamiltonian functions for the corresponding regions. The Hamiltonian functions are constant and equal to zero because the Lagrange functions [Eq. (A13)] do not depend on s and the arc lengths of the regions are not fixed.

The Euler-Langrange equations show that F_i ($i = 1$, 2, and 3) are constants. Moreover, the multiplicators F_1 and F_2 equal zero, because the lengths of the corresponding regions along the symmetry axis are not fixed.

The first five terms in Eq. (A15) lead to the relations between the curvatures at the boundaries B, C, D, and E by taking into consideration the continuity of the Hamiltonian functions [Eq. (A16)]. Then the corresponding boundary conditions can be written in the following forms [8]:

$$c_m|_{B-} = \frac{c_m|_{B+} - c_m|_{E-}}{2} - \sqrt{2W}, \qquad \text{(A17)}$$

$$c_m|_{C+} = \frac{c_m|_{C-} - c_m|_{D+}}{2} - \sqrt{2W}, \qquad \text{(A18)}$$

$$c_m|_{D-} = \frac{c_m|_{D+} - c_m|_{C-}}{2} - \sqrt{2W}, \qquad \text{(A19)}$$

$$c_m|_{E+} = \frac{c_m|_{E-} - c_m|_{B+}}{2} - \sqrt{2W}, \qquad \text{(A20)}$$

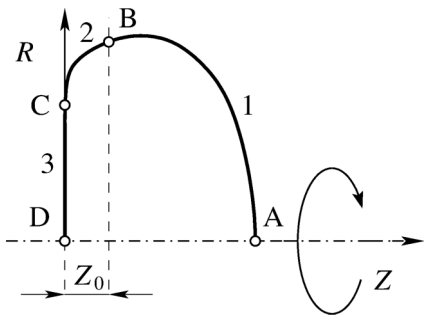

FIG. 10. Schematic presentation of an axisymmetric vesicle stuck to the plane because of the square well potential with Z_0 being the interaction distance. The free, interaction, and stuck regions are denoted by numerals (1, 2, and 3), whereas the boundaries of these regions are denoted by letters (A, B, C, and D).

where $c_m|_{B+}$, $c_m|_{C-}$, $c_m|_{D+}$, $c_m|_{E-}$, $c_m|_{B-}$, $c_m|_{E+}$, $c_m|_{C+}$ and $c_m|_{D-}$ are curvatures along the meridians at the rims of the double bilayer region and at the rims of the polar and equatorial regions with this region, respectively.

Since the variations δr, $\delta\psi$, and δz at the boundaries of the adhesion region are independent, Eq. (A15) leads to

$$\Gamma|_{C-} - \Gamma|_{D+} = \Gamma|_{C+} - \Gamma|_{D-}, \qquad \text{(A21)}$$

$$\Gamma|_{E-} - \Gamma|_{B+} = \Gamma|_{E+} - \Gamma|_{B-}, \qquad \text{(A22)}$$

where $\Gamma|_{B-}$, $\Gamma|_{C-}$, $\Gamma|_{C+}$, $\Gamma|_{D-}$, $\Gamma|_{E-}$, and $\Gamma|_{E+}$ are the transfer shear forces in a radial direction. Other boundary conditions in expression (A15) determine the smoothness and continuity of the membrane.

The system of differential equations [Eqs. (A14)] is solved using the shooting method. The values for M_i, L, F_3, the initial radii at points B and C, and the initial meridian curvature at the two vesicle poles and the points B and C (10 parameters) are tuned such that the boundary conditions are fulfilled and the vesicle volumes, the total membrane area and equilibrium area difference assume their given values.

APPENDIX B: THE SQUARE WELL INTERACTION FOR THE CONFORMATION OF PHOSPHOLIPID VESICLES

By minimizing the mechanical energy, the equilibrium shapes for the vesicle membrane considering the square well interaction can be obtained (Fig. 10). Using the dimensionless units (Appendix A), for a given vesicle volume and the membrane area the extremes of the mechanical energy in this case correspond to the stationary points of the functional

$$\tilde{g} = e_b + e_{\tilde{w}} - Mv + La. \qquad \text{(B1)}$$

The membrane interaction energy in relative units is given by $e_{\tilde{w}} = E_{\tilde{w}}/8\pi k_c$ where $E_{\tilde{w}}$ is defined in the main text [Eq. (7)]. The reduced local bending energy, the reduced vesicle volume, the reduced membrane area, and the Lagrange multipliers (e_b, v, a, M, and L) are defined in Appendix A. Using the parametrization of the contour (Appendix A) four points on the contour with respect to the region boundaries are introduced: point A is the starting point, which lies at the pole of the vesicle; point B is at the rim between the free and

interaction region; point C is at the rim between the interaction and stuck region; and point D is the ending point, which lies at the opposite pole of the vesicle (Fig. 10). Using integral expressions for v and a (Appendix A), we can express the variation of the functional $\tilde{g}$ with respect to the shape as

$$\delta\tilde{g} = \delta\int_A^B \mathcal{L}_1\, ds + \delta\int_B^C \mathcal{L}_2\, ds + \delta\int_C^D \mathcal{L}_3\, ds, \tag{B2}$$

where the Lagrangian functions (considering the interrelations between the parametrization variables) can be written as

$$\mathcal{L}_i = \frac{r}{8}\left(\frac{\sin\psi}{r} + \dot{\psi}\right)^2 - (1.5 - |i - 2.5|)\tilde{W}\frac{r}{2} - M\frac{3r^2\sin\psi}{4} + L\frac{r}{2} + \Gamma(\dot{r} - \cos\psi) - F_i(\dot{z} + \sin\psi). \tag{B3}$$

The index i is 1, 2, and 3 when referring to the free, interaction, and stuck region, respectively.

The variation of $\delta\tilde{g}$ leads to the system of the differential equations, which is similar to Eqs. (A14). In the system the parameter $W/2$ has to be replaced by $\tilde{W}$ since in the variation of functional g [Eq. (A12)] the adhesion interaction is taken into account twice. The boundary conditions obtained by the minimization are

$$-H_1\delta s\big|_A^B - H_2\delta s\big|_B^C - H_3\delta s\big|_C^D + \sum_j \frac{\partial\mathcal{L}_1}{\partial\dot{x}_j}\delta x_j\big|_A^B + \sum_j \frac{\partial\mathcal{L}_2}{\partial\dot{x}_j}\delta x_j\big|_B^C + \sum_j \frac{\partial\mathcal{L}_3}{\partial\dot{x}_j}\delta x_j\big|_C^D = 0, \tag{B4}$$

where $\mathbf{x}$ is the vector of variables and H_i are the Hamiltonian functions for the corresponding regions. The multiplicator F_1 is zero because the distance of the pole A from the reference plane is not fixed, whereas the value of F_2 is generally a nonzero constant because the interaction distance is fixed. Due to the same reasons as in Appendix A, the Hamiltonian functions H_1 and H_2 are equal to zero. Consequently, expression (B4) leads to the boundary condition at point C:

$$2F_2\sin\psi|_C + \tilde{W}r|_C = 0, \tag{B5}$$

which determines the interrelation between the adhesion and the vesicle parameters. Large adhesion causes a large force in the axial direction (F_2). Additionally, expression (B4) determines the continuity and smoothness of the membrane, and the continuity of the membrane curvatures and of the transfer shear forces in a radial direction.

[1] B. Alberts, D. Bray, J. Lewis, M. Raff, K. Roberts, and J. D. Watson, *Molecular Biology of the Cell* (Garland, New York, 1994).

[2] A. Hategan, K. Sengaputa, S. Kahn, E. Sackmann, and D. E. Discher, Biophys. J. **87**, 3547 (2004).

[3] U. Seifert and R. Lipowsky, Phys. Rev. A **42**, 4768 (1990).

[4] S. Pierrat, F. Brochard-Wyart, and P. Nassoy, Biophys. J. **87**, 2855 (2004).

[5] P. Ziherl and S. Svetina, Proc. Natl. Acad. Sci. USA **104**, 761 (2007).

[6] E. Evans, Biophys. J. **31**, 425 (1980); **48**, 175 (1985).

[7] T. Mareš, M. Daniel, A. Iglič, V. Kralj-Iglič, and M. Fošnarič, Sci. World J. **2012**, 146804 (2012).

[8] J. Derganc, B. Božič, S. Svetina, and B. Žekš, Biophys. J. **84**, 1486 (2003).

[9] R. Lipowsky and U. Seifert, Langmuir. **7**, 1867 (1991).

[10] H. I. Petrache, N. Gouliaev, S. Tristram-Nagle, R. Zhang, R. M. Suter, and J. F. Nagle, Phys. Rev. E **57**, 7014 (1998).

[11] S. Svetina and B. Žekš, Eur. Biophys. J. **17**, 101 (1989).

[12] U. Seifert, K. Berndl, and R. Lipowsky, Phys. Rev. A **44**, 1182 (1991).

[13] W. Wintz, H.-G. Döbereiner, and U. Seifert, Europhys. Lett. **33**, 403 (1996).

[14] H. J. Deuling and W. Helfrich, J. Phys. (Paris) **37**, 1335 (1976).

[15] A.-S. Smith, E. Sackmann, and U. Seifert, Phys. Rev. Lett. **92**, 208101 (2004).

[16] X.-H. Zhou, J.-L. Liu, and S.-L. Zhang, Colloids Surf. B **110**, 372 (2013).

[17] J. Steinkühler, J. Agudo-Canalejo, R. Lipowsky, and R. Dimova, Biophys. J. **111**, 1454 (2016).

[18] J. Majhenc, B. Božič, S. Svetina, and B. Žekš, Biochim. Biophys. Acta **1664**, 257 (2004).

[19] A. Iglič, V. Kralj-Iglič, B. Božič, M. Bobrowska-Hägerstrand, B. Isomaa, and H. Hägerstrand, Bioelectrochemistry **52**, 203 (2000).

[20] J. P. Reeves and R. M. Dowben, J. Cell. Physiol. **73**, 49 (1969).

[21] B. Božič and J. Majhenc, ChemPhysChem **10**, 2862 (2009).

[22] W. Helfrich, Z. Naturforsch. C **28**, 693 (1973).

[23] S. Svetina, M. Brumen, and B. Žekš, Stud. Biophys. **110**, 177 (1985); B. Božič, S. Svetina, B. Žekš, and R. E. Waugh, Biophys. J. **61**, 963 (1992); L. Miao, U. Seifert, M. Wortis, and H.-G. Döbereiner, Phys. Rev. E **49**, 5389 (1994); E. Evans and A. Yeung, Chem. Phys. Lipids **73**, 39 (1994).

[24] R. E. Waugh, J. Song, S. Svetina, and B. Žekš, Biophys. J. **61**, 974 (1992); R. M. Raphael and R. E. Waugh, *ibid.* **71**, 1374 (1996); S. Svetina, B. Žekš, R. E. Waugh, and R. M. Raphael, Eur. Biophys. J. **27**, 197 (1998); S. Svetina and B. Žekš, in *Nonmedical Applications of Liopsomes*, edited by D. D. Lasic and Y. Barenholz (CRC, Boca Raton, FL, 1996), p. 13.

[25] U. Seifert, Eur. Phys. J. B **8**, 405 (1999).

[26] E. Evans, W. Rawicz, and B. A. Smith, Faraday Discuss. **161**, 591 (2013).

[27] In practice a vesicle cannot change its shape immediately, because the membrane and the water inside and outside of the vesicle cannot be rearranged promptly.

[28] R. Capovilla and J. Guven, J. Phys. A **35**, 6233 (2002).

[29] R. Lipowsky and S. Leibler, Phys. Rev. Lett. **56**, 2541 (1986).

[30] R. Lipowsky and B. Zielinska, Phys. Rev. Lett. **62**, 1572 (1989).

[31] F. Jülicher and U. Seifert, Phys. Rev. E **49**, 4728 (1994).